AD-760 039

POSSIBLE CONDENSATION IN ROCKET EXHAUST PLUMES II

Benjamin J. C. Wu

Yale University

Prepared for:

Advanced Research Projects Agency

April 1973

DISTRIBUTED BY:

NTIS

National Technical Information Service
U. S. DEPARTMENT OF COMMERCE
5285 Port Royal Road, Springfield Va. 22151

AD 760039

SPECIAL TECHNICAL REPORT
April 1973

POSSIBLE CONDENSATION IN ROCKET EXHAUST PLUMES II

Benjamin J.C. Wu

DDC
RETURN
REPRODUCED
D

The views and conclusions contained in this document are those of the author and should not be interpreted as necessarily representing the official policies, either expressed or implied, of the Advanced Research Projects Agency or the U.S. Government.

Sponsored by:
Advanced Research Projects Agency
ARPA Order Nr. 1179

Principal Investigator Prof. P.P. Wegener
Contract Number DAAH01-73-C-0442
Duration of Contract 2/1/73 to 12/31/73
Amount of Contract $30,000.00
Phone Number (203) 436-8674

DISTRIBUTION STATEMENT A
Approved for public release;
Distribution Unlimited

DEPARTMENT OF ENGINEERING
AND APPLIED SCIENCE

YALE UNIVERSITY

Reproduced by
NATIONAL TECHNICAL
INFORMATION SERVICE
U S Department of Commerce
Springfield VA 22151

14. KEY WORDS	LINK A		LINK B		LINK C	
	ROLE	WT	ROLE	WT	ROLE	WT
Condensation						
Nucleation						
Droplet growth						
Rocket exhaust						

Security Classification

DOCUMENT CONTROL DATA - R & D

(Security classification of title, body of abstract and indexing annotation must be entered when the overall report is classified)

1. ORIGINATING ACTIVITY (Corporate author)
Department of Engineering and Applied Science
Yale University

2a. REPORT SECURITY CLASSIFICATION

2b. GROUP

3. REPORT TITLE

POSSIBLE CONDENSATION IN ROCKET EXHAUST PLUMES II

4. DESCRIPTIVE NOTES (Type of report and inclusive dates)
Special Technical Report April 1973

5. AUTHOR(S) (First name, middle initial, last name)

Benjamin J.C. Wu

6. REPORT DATE	7a. TOTAL NO. OF PAGES	7b. NO. OF REFS
April 1973	~~41~~ 44	13

8a. CONTRACT OR GRANT NO.	9a. ORIGINATOR'S REPORT NUMBER(S)
DAAHOI-73-C-0442	
b. PROJECT NO.	
c.	9b. OTHER REPORT NO(S) (Any other numbers that may be assigned this report)
d.	

10. DISTRIBUTION STATEMENT
Distribution unlimited.

11. SUPPLEMENTARY NOTES	12. SPONSORING MILITARY ACTIVITY
	Advanced Research Projects Agency of the Department of Defense

13. ABSTRACT The results of a computational study of one aspect of condensation in the exhaust plume consisting of H_2O and H_2 of an Apollo rocket engine are reported. Saturation of water vapor occurs at about 225°K in the plume. Hydrogen remains unsaturated in the given flow field. Under the assumption of steady state nucleation, onset of H_2O condensation by homogeneous nucleation is estimated to occur at x=47, 40, and 13 m, i.e., about 45, 38, and 13 m downstream of the nozzle exit plane, along $\theta=\bar{0}.\bar{0}$, 0.3, and 0.8 stream tubes, respectively. It is further estimated that at x=150 m along the center stream tube a cloud of 10^{10} H_2O droplets/cm^3 is formed. The mass mean radius of this cloud of droplets is about 17 Å, and there are only about 1/100 as many droplets with r=14 Å or 21 Å as with r=17 Å.

It must be emphasized that the fundamental assumption of steady state nucleation, on which the above conclusions are based, appears to be questionable for this problem. The flow is too fast for the steady state nucleation rate to be attained. Consequently, H_2O condensation by homogeneous nucleation may be delayed or even inhibited in this exhaust plume.

However, we must remember that homogeneous nucleation is by no means the only mechanism that can induce H_2O condensation. Earlier condensation may be initiated by the processes of heterogeneous and binary nucleation. These processes are being studied at present.

DD FORM 1 NOV 68 1473

Unclassified
Security Classification

ACKNOWLEDGEMENTS

The author wishes to thank Professor Peter P. Wegener for his cooperation in this work. The computer programs used in this study were developed in recent years at Yale University as part of the research in homogeneous nucleation sponsored by the Power Branch of the Office of Naval Research. The author acknowledges the courtesy of AeroChem Research Laboratories for permission to use an earlier report as a supplement to this report.

CONTENTS

LIST OF TABLES

LIST OF FIGURES

I INTRODUCTION

The results of a computational study of one aspect of condensation phenomena in the high altitude exhaust plume of an Apollo rocket engine are presented here. The exhaust gas consists of water vapor and hydrogen. The objective of this study is to determine whether any of the species is likely to condense. and if so, at what location in the plume the onset of condensation may be expected.

Only the possibilities of condensation by the process of homogeneous nucleation have been studied. The effects of the other processes which may induce condensation, namely, binary nucleation and heterogeneous nucleation have not yet been studied for this investigation.

In addition to nucleation the average growth of droplets was calculated beyond the point of onset of condensation and finally a rough estimate of the droplet size distribution far downstream of the onset point has been made.

The general method of calculation is the same as that employed in an earlier study of the exhaust plume of a different rocket engine (Wu 1972).* The method will therefore not be reiterated here in detail.

Tables I - IV summarize the flow variables of the exhaust plume in three stream tubes designated as ϑ = 0.0, 0.3, and 0.8 radians as transmitted to us by Teare (1972)

* Note references at the end as listed alphabetically by senior author. Moreover, because of the constant reference to the earlier report (Wu 1972), it is reproduced here, by permission of AeroChem Research Laboratories, Inc., Princeton, N.J., as a supplement to this report.

of AVCO-Everett Research Laboratory. The first data point given for each stream tube corresponds to the location of the exit of the rocket nozzle. As before, it was suggested to us that the flow field is chemically frozen in the region of the given data. Hence the law of mass conservation can be applied to H_2O and H_2 independently. In the absence of appreciable condensation, the partial pressures of the species are easily computed by taking the mole fractions of the species to be constant. Figure (1) shows the variation of the total and partial pressures of the species with temperature along the center stream tube ($\theta = 0.0$). The location on the stream tube is not marked. The pressure - temperature functions for the other two stream tubes are practically indistinguishable from those in Fig. (1). The saturation vapor pressure, $p_{\infty H_2O}(T)$, of water is also plotted in Fig. (1). The intersection of the saturation line with the partial pressure curve marks the state at which the water vapor in the exhaust becomes saturated. This location occurs at $x = 3220$ cm on the center stream tube which is about 3050 cm beyond the exit plane. The saturation conditions on all three stream tubes are summarized in Table V. The lowest temperature in the given flow field is 69°K. Since the critical temperature of hydrogen, 43°K, is still lower, this vapor remains unsaturated in the exhaust.

The effective molecular weight and ratio of specific heats of the exhaust gas, computed under the assumptions of chemically frozen, isentropic flow, are

$$\mu = 13.102 ,$$

and

$$1.217 < \gamma < 1.351 \quad .$$

As in the previous case, the value of γ varies somewhat along the stream tube. However, for $69 < T < 225°K$, γ remains practically constant at 1.351 for all three stream tubes. Since the condensation calculations would involve only the flow region in which the gas temperature falls in this limited range, it was decided to use the value $\gamma = 1.351$ in the calculation of the entire flow field until the point where appreciable condensation has noticeably altered the gas phase composition.

With the molecular weight and ratio of specific heats known, the supply conditions* of a "fictitious reservoir", p_o and T_o, and the area distribution* of a "fictitious nozzle" are easily computed using the data in Tables I - IV and the equations of one-dimensional isentropic flow of ideal gases. The values of these parameters are listed in Table VI, and they are used as the input to the computer programs. It should be pointed out that the use of these "fictitious parameters" is only practical for calculations. The parameters associated with the fictitious nozzle and reservoir used here have no bearing on the actual rocket nozzle and supply chamber conditions. It is noted that a simple square law

$$A/A^* = C\, x^2 \qquad (1)$$

---

* These quantities are calculated to facilitate subsequent computations, see pp. 9-11 of Wu (1972) for details.

and

$$1.217 < \gamma < 1.351 \quad .$$

As in the previous case, the value of γ varies somewhat along the stream tube. However, for $69 < T < 225^{\circ}K$, γ remains practically constant at 1.351 for all three stream tubes. Since the condensation calculations would involve only the flow region in which the gas temperature falls in this limited range, it was decided to use the value $\gamma = 1.351$ in the calculation of the entire flow field until the point where appreciable condensation has noticeably altered the gas phase composition.

With the molecular weight and ratio of specific heats known, the supply conditions* of a "fictitious reservoir", p_o and T_o, and the area distribution* of a "fictitious nozzle" are easily computed using the data in Tables I - IV and the equations of one-dimensional isentropic flow of ideal gases. The values of these parameters are listed in Table VI, and they are used as the input to the computer programs. It should be pointed out that the use of these "fictitious parameters" is only practical for calculations. The parameters associated with the fictitious nozzle and reservoir used here have no bearing on the actual rocket nozzle and supply chamber conditions. It is noted that a simple square law

$$A/A^* = C\, x^2 \qquad (1)$$

---

* These quantities are calculated to facilitate subsequent computations, see pp. 9-11 of Wu (1972) for details.

is used to describe the area variation along each stream tube. This is an accurate correlation for the part of the stream tube where the condensation calculations will be made, as seen in Figure (2).

The mass fraction of the condensate is computed by integrating the equation (see, e.g. Wegener and Mack 1958)

$$g(x) = \frac{4\pi\rho_c}{3m} \int_{-\infty}^{x} J(\zeta)A(\zeta)r^3(x,\zeta)d\zeta \quad . \tag{2}$$

Here, $r(x,\zeta)$ is the final radius of a droplet initially formed at ζ by homogeneous nucleation and having undergone growth before reaching the point x downstream of ζ. This radial growth is expressed formally by

$$r(x,\zeta) = r^*(\zeta) + \int_{\zeta}^{x} \frac{dr}{dx}\, d\zeta \quad , \tag{3}$$

where dr/dx is the droplet growth rate. In addition, $J(\zeta)$ is the homogeneous nucleation rate of critical clusters taken to be

$$J = \Gamma\, J_{class} \quad , \tag{4}$$

where Γ is an empirical correction factor and the value of J_{class} is the rate to be computed from the so-called classical theory of homogeneous nucleation. With a proper choice of Γ, we avoid the difficulties involved in calculating J, caused by our lack of knowledge of the surface tension of small

systems and the uncertainties in nucleation theory. The droplet growth rate is computed from the free molecular equation as discussed in the previous report (Wu 1972), since again the droplet radii are much smaller than the vapor mean free path.

II RESULTS AND DISCUSSIONS

As a direct check on the input data to the computer programs, the computed pressure - temperature relation along the center stream tube near the saturation point of water vapor, together with the initially given data points are plotted in Figure 3. The agreement is seen to be good.

Figure (4) shows the accummulation of H_2O condensate mass fraction $g \equiv \dot{m}_c/\dot{m}$ along the center stream tube as a function of the empirical correction factor Γ here indicated in powers of ten. The qualitative feature of an onset of condensation is clearly exhibited in these curves with the appearance of the condensate as a sudden process. This qualitative feature is well verified in many observations and it does not depend on the choice of Γ. The flow time of fluid elements originating at H_2O saturation is shown by the time of flight scale at the bottom of this figure. Defining the onset of condensation* as the point where the mass fraction of condensate $g = 10^{-3}$, we plot the calculated point of onset in the center stream tube in Fig. (5) again as a function of the correction factor Γ. Similar results for the flow in the other two stream tubes are shown in Figures (6) and (7).

The lower limit of Γ is likely to be of the order one, which corresponds to the homogeneous nucleation rate given by the classical theory.

---

* The choice of this definition has been discussed in detail in the previous report (Wu 1972).

On the other limit, the theoretical value of Γ is estimated to be

$$\Gamma = \frac{\tilde{q}_{tr}^{*} \, q_{rot}^{*}}{q_{rep}^{*}} = 10^{14}$$

where q_{rep}^{*}, the replacement factor, is given the value 10^3 as proposed by Lothe and Pound (1962) in their statistical mechanical model. The translational and rotational partition functions, $\tilde{q}_{tr}^{*}$ and q_{rot}^{*}, are computed from well known formulas from statistical mechanics (e.g. Wegener and Parlange 1970). This latter value of Γ is much higher than the empirical estimate, a discrepancy between Lothe and Pound's theory and experiments found before at higher temperatures. Other models for q_{rep}^{*} (e.g. Dunning 1965) yield values of Γ that are much lower. However, none of the theories proposed are yet in a state to be applicable to engineering estimates. We note in Figure (5) that the range $1 < \Gamma_{theory} < 10^{14}$ corresponds to the range $41 < x_{onset} < 55$ m calculated for steady-state homogeneous nucleation theories in the center stream tube. In view of this uncertainty, we shall use empirical knowledge gained in previous experiments with condensation in nozzles.

For this work, therefore, the choice $\Gamma = 10^6$, $\sigma = \sigma_{ice} = 96$ dyne/cm and $\alpha = 1.0$ has again been made to estimate the onset of condensation of H_2O. The motivation for this assumption for the empirical correction has been further elaborated in Wu (1972). The choice of these values was

based on experiments where the mole fraction of the condensing vapor y << 1. In this nozzle, however, we have $y_{H_2O} = 0.6929$, a high value that necessitates an examination of the non-isothermal kinetics of nucleation.

The so-called non-isothermal effect in homogeneous nucleation was first noted by Kantrowitz (1951), treated in detail by Feder et al. (1966), and applied to condensation in steam nozzle flows by Barschdorff et al. (1972). It deals with the fact that the clusters are generally not at the same temperature as the surrounding gas, and that the latent heat of condensation added to a cluster when it is growing towards the critical size must be dissipated to the surrounding gaseous medium. This heat transfer process is coupled with the growth of the clusters and results in a slower growth rate of clusters to their critical size. The nucleation rate will in turn be retarded due to the transfer of latent heat. Hence, one expects the non-isothermal nucleation rate to be lower than the isothermal nucleation rate given by the classical theory. When the vapor is carried in a large quantity of inert diluent which participates in heat transfer, the non-isothermal nucleation rate may approach the isothermal rate. The non-isothermal nucleation theory of Feder et al. (1966) has recently been examined by Wilemski (1973) who found that the assumptions made by Feder et al. are indeed reasonable and their theory is applicable to this work. A simple calculation using the results of Feder et al. (1966) reveals that

for $$J_{noniso} = \frac{b^2}{b^2+q^2} J_{iso} ,$$

we have

$$0.02 < \frac{b^2}{b^2+q^2} < 0.024 ,$$

for $3250 < x < 4680$ cm in the center stream tube. The quantities b and q are defined in terms of the thermodynamic state of the supersaturated vapor and the inert carrier gas, and applicable expressions for these quantities can be found in Wu (1972). Hence, the non-isothermal nucleation factor is found to be nearly a constant of the order of 10^{-2}. In other words, the non-isothermal nucleation is only about 1/100 of the standard one. As before, we estimate that the proper value of Γ for the problem being considered should lie between 10^4 and 10^6. Moreover, it is implied throughout that the assumptions underlying the steady-state theory of homogeneous nucleation are valid. From these calculations, we finally find that condensation of water vapor may be expected in the plume at

$x \approx 47$ m for $\theta = 0.0$ stream tube,
$x \approx 40$ m for $\theta = 0.3$ stream tube, and
$x \approx 13$ m for $\theta = 0.8$ stream tube.

These x-coordinates correspond roughly to 45, 38, and 13 m downstream of the nozzle exit plane along $\theta = 0.0$, 0.3, and 0.8 stream tubes, respectively.

The thermodynamic conditions at the onset of condensation computed for the three stream tubes assuming $\Gamma = 10^5$ are summarized in Table VII. Moreover, the onset condition in the center stream tube is compared with available experimental results in Fig. (8). It is again noted that the temperature and vapor pressure at the onset of condensation are still much lower than the range of states for which experiments are available. However, the pressures are higher than those found in the previous case (Wu 1972) where $P_{H_2O} = 10^{-3}$ torr at the onset with T ~ 150°K. It is our opinion, however, that extrapolation of our empirical knowledge on Γ to the temperatures and pressures occurring in this problem is not unreasonable. We shall see later that there are sources for more serious uncertainties, which may outweigh the uncertainties stated so far.

Under the assumption that the stream tube area variation is not affected by the latent heat addition to the gas stream resulting from condensation, calculations of droplet growth beyond the onset point can be made with the available computer programs. The results of such a calculation are shown in Figure 9. Here, $\bar{r}$ is the mass mean radius of all the droplets present , i.e., the spherical radius resulting from evenly distributing the total mass of condensate over all the droplets present. Thus,

$$\bar{r} = \left(\frac{3g\rho}{4\pi N \rho_c} \right)^{1/3} ,$$

where ρ is the density of the vapor-carrier gas mixture and N is the total number of droplets present. The droplet size distribution was calculated by following the growth process of particular classes of droplets as they are carried downstream by the gas flow. Each class consists of droplets formed at a particular location, ζ, along the stream tube. Hence, an observer located somewhere, x, downstream of this location will see a total of $J(\zeta)\, A(\zeta)\, d\zeta$ droplets in this class flying by per unit time. All of the droplets in this class will have radii between r and r + dr, where r is given by Eq. (3), and dr is related to $d\zeta$. Because the nucleation zone is quite narrow, the cross-sectional area of the stream tube does not change much in this particular zone and the number of droplets in different classes will be roughly proportional to the nucleation rates, $J(\zeta)$, at the respective "birth places" of the classes of droplets.

Hence, the class having the largest number of droplets must be formed at the location where J is at its maximum. In the center stream line, with the assumption $\Gamma = 10^5$, J_{max} occurs at x = 4700 cm. The radii of droplets formed at x = 4700 cm [i.e. r(4700, x)] practically coincides with $\bar{r}$ for x > 4900 cm. This means that the "peak" in the droplet size distribution coincides with the mass mean radius of all droplets present. This qualitative feature is well established by laser light scattering experiments with water vapor (Wegener and Stein 1969) and with ethyl alcohol by Clumpner (1971).

Four more curves, r(4440, x), r(4540, x), r(4880, x)

and r(4940, x) are also shown in Fig. 9. The nucleation rates calculated at these points satisfy the following relation:

$$J(4700) : J(4880) : J(4940) = J(4700) : J(4540) : J(4440)$$
$$= 1 : 0.1 : 0.01 \quad .$$

Consequently, one estimates that if the assumptions underlying these calculations are valid, there will be ten times fewer droplets in the classes r(4880, x) and r(4540, x) than in the class r(4700, x) which has the largest number of droplets. Similarly, there will be one hundred times fewer droplets in the classes r(4940, x) and r(4440, x) than the class r(4700, x). In other words, we estimate that at x = 150 m in the center stream tube, the mass mean radius of all the droplets is 17 Å and this happens to be the "most probable" size of the droplets. An H_2O droplet of this size contains about 600 molecules. At this size, macroscopic notions like surface tension are probably meaningful. Furthermore, we estimate that the numbers of droplets with r = 15 Å and 20 Å are only 1/10 of that of 17 Å and those of 14 Å and 21 Å are only 1/100 of the number of droplets with r = 17 Å. The total number density of droplets of all sizes, computed from

$$N(x) = \frac{\rho(x)}{m} \int_{-\infty}^{x} J(\zeta)A(\zeta)d\zeta \quad ,$$

is found to be in the order of 10^{10} cm^{-3} at x = 150 m.

We must now discuss the weakest link in the above analysis; all the above calculations are based on the fundamental assumption of a steady-state homogeneous nucleation process. A careful examination of the thermodynamic state and flow variables in the supersaturated region reveals, however, that this assumption may not be valid. The flow time, τ_f, from saturation to onset calculated for $\Gamma = 10^5$ is about 3 msec along the center stream tube as the bottom scale in Fig. 4 indicates. The build-up time, τ_r, for steady-state homogeneous nucleation under the existing thermodynamic conditions, calculated using the ideas of Kantrowitz (1951), is about 14 msec. The appropriate Damköhler parameter, $D \equiv \tau_f/\tau_r$ is therefore $D \approx 0.2$ or $D < 1$ in the exhaust plume being considered. A typical value for D found for condensation of ethanol in the nozzle used by Wegener et al. (1972) is of the order 10^2. The condition $D > 1$ must be satisfied in order that the steady state cluster distribution may be established when the thermodynamic state of the vapor is changing. As in the previous case, we found here that there is probably not enough time for the steady state nucleation rate to be attained. The actual homogeneous nucleation rate may therefore be lower than the steady-state rate used in the calculations here. Hence, a calculation involving non-steady homogeneous nucleation rate may yield onset of H_2O condensation further downstream from that found in this work, or it may predict no condensation at all. At any

rate, condensation by homogeneous nucleation would most likely not occur upstream of the onset locations found here.

III SUMMARY AND CONCLUSIONS

Possible condensation by homogeneous nucleation is investigated for the exhaust plume of an Apollo rocket engine. The exhaust studied consists of a chemically frozen mixture of H_2O and H_2. Water vapor becomes saturated at about 225°K in the exhaust and subsequent expansions to lower temperatures may lead to its condensation. Hydrogen remains unsaturated in the region for which the flow field is given.

Onset of water vapor condensation induced by homogeneous nucleation has been calculated assuming steady-state nucleation theory for non-isothermal cluster growth and using empirical information gathered in numerous previous studies at higher temperatures and pressures. The results of this calculation show that H_2O condensation will take place at about 170°K, which is approximately 45, 38, and 13 m downstream of the nozzle exit plane for θ = 0.0, 0.3, and 0.8 radian stream tubes, respectively. In the center stream tube (θ = 0.0), calculations of the condensation process beyond the onset point, using the stream tube area distribution of noncondensing flow lead to an estimate of the droplet size distribution. It is estimated that at x = 150 m in the center stream tube, about 10^{10} droplets/cm^3 are formed by homogeneous nucleation. The mass mean radius of this cloud of droplets is about 17 Å. This is also the size of the largest number of droplets, i.e. the size distribution is quite "narrow". There are only 1/10 as many droplets

with r = 15 Å and 20 Å as droplets with r = 17 Å, and 1/100 with r = 14 Å and 21 Å. There are about 600 H_2O molecules in a droplet with r = 17 Å.

It must be emphasized that the above conclusions are derived from the crucial assumption of steady-state homogeneous nucleation. A further examination of the flow field reveals that this assumption does not appear to be valid for the problem at hand. The build-up time for steady state homogeneous nucleation is estimated to be 14 msec while the relevant flow time is only about 3 msec. Thus, it is seen that the flow is probably too rapid for the steady state nucleation rate to be achieved. Consequently, H_2O condensation induced by homogeneous nucleation, as summarized in the preceeding paragraph may occur at locations farther downstream than estimated or it may not occur at all. On the other hand, condensation by homogeneous nucleation cannot be ruled out at the present time since the steady state theory provides only one limit for its occurrence.

We must finally emphasize that homogeneous nucleation is not the only mechanism capable of initiating H_2O condensation. The processes of heterogeneous and binary nucleation are also possible and these mechanisms both favor early phase change. Work in these directions is currently being carried out at Yale since it is required to assess the probability of condensation caused by heterogeneous or binary nucleation.

LIST OF SYMBOLS

a	speed of sound.
A	cross sectional area.
g	mass fraction of condensate.
J	nucleation rate.
$\dot{m}$	mass flow rate in the nozzle.
M	Mach number.
n	number of molecules in a cluster.
N	number density of clusters.
p	pressure.
p_∞	saturation vapor pressure over a flat surface.
q_{rep}	replacement factor.
$\tilde{q}_{tr}$, q_{rot}	translational and rotational partition functions.
r	radius.
s	saturation ratio ($= p_v/p_\infty$).
t	time.
T	temperature.
u	velocity.
x	coordinate along flow direction.
y	mole fraction.
α	mass accommodation coefficient.
γ	ratio of specific heats.
Γ	empirical factor.
μ	molecular weight.
ρ	mass density.
σ	surface tension (or surface free energy).
τ_f	characteristic flow time.

τ_r relaxation time for steady-state nucleation.

ω mass fraction of vapor.

Subscripts

c condensate.

class classical.

i inert carrier gas.

noniso nonisothermal.

o initial supply (stagnation) conditions.

r a cluster of radius r.

v condensable vapor.

∞ flat surface.

Superscript

* cluster of critical size, or nozzle throat.

V REFERENCES

D. Barschdorff, W.J. Dunning, P.P. Wegener, and B.J.C. Wu (1972) Nature - Physical Science, 240, 166.

J.A. Clumpner (1971) J. Chem. Phys., 55, 5042.

W.J. Dunning (1965) Adsorption et Croissance Cristalline, Colloques Internationaux du Centre National de la Recherche Scientifique, No. 152, p. 369, CNRS, Paris.

J. Feder, K.C. Russell, J. Lothe and G.M. Pound (1966) Adv. Phys., 15, 111.

G. Gyarmathy and H. Meyer (1965) VDI - Forschungsheft 508.

A. Kantrowitz (1951) J. Chem. Phys., 19, 1097.

J. Lothe and G.M. Pound (1962) J. Chem. Phys., 36, 2080.

A.A. Pouring (1963) D. Eng. Thesis, Yale University, New Haven, Conn.

R. Roberts (1969) Report 97, Gas Turbine Laboratory, Massachusetts Institute of Technology, Cambridge, Mass.

G.D. Stein (1967) PhD Thesis, Graduate School, Yale University, New Haven, Conn.

J.D. Teare (1972) AVCO - Everett Research Laboratory, Private communication.

P.P. Wegener and L.M. Mack (1958) in Advances in Applied Mechanics, H.L. Dryden, T. von Karman eds., 5, 307, Academic Press, N.Y.

P.P. Wegener and J.-Y. Parlange (1970) Naturwiss., 57, 525.

P.P. Wegener and G.D. Stein (1969) Twelfth Symposium (International) on Combustion, the Combustion Institute, Pittsburgh, Pa., p. 1183.

P.P. Wegener, J.A. Clumpner, and B.J.C. Wu (1972) Phys. Fluids, 15, 869.

G. Wilemski (1973) Yale University, Private communication.

B.J.C. Wu (1972) Report prepared for AeroChem Research Laboratories, Inc., Princeton, N.J. under contract F04611-72-C-0013 (J.98) Dept. of Eng. and Applied Sci., Yale University. Reproduced as a supplement to the report at hand.

Table I

SPECIFICATIONS FOR CONDENSATION CALCULATION II

Initial conditions for 3 stream tubes:

$T = 1417°K$

$p = 125.4$ torr

$\rho = 1.860 \times 10^{-5}$ g/cm^3

$u = 4.170 \times 10^{-5}$ cm/sec

Area = 3.010 cm^2

$[H_2O] = .6929$
$[H_2] = .3071$ } mole fractions

All three stream tubes have same initial gas properties at area A = 3.01 cm^2 but expansion to A ≈ 3 x 10^4 cm^2 occurs over different axial distances:

$\theta = 0$	$169.5 \leq x \leq 17320$ cm
$\theta = 0.3$	$143.8 \leq x \leq 14590$ cm
$\theta = 0.8$	$46.79 \leq x \leq 4793$ cm

Table II

θ = 0.0 Radians

x(cm)	p	T	ρ	u	A
169.5	125.4	1417	1.86×10^{-5}	4.17×10^{5}	3.010
199.7	83.37	1311	1.33	4.254	4.108
235.9	54.51	1202	9.53×10^{-6}	4.332	5.655
277.7	35.89	1101	6.849	4.401	7.745
325.7	23.78	1009	4.978	4.463	1.055×10^{1}
396.2	14.37	900.5	3.353	4.531	15.37
480.5	8.717	803.3	2.281	4.590	22.30
603.5	4.805	698.4	1.446	4.652	34.72
756.0	2.655	605.4	9.214×10^{-7}	4.704	53.86
1017	1.207	498.5	5.087	4.762	96.38
1417	0.4980	398.6	2.024	4.815	1.848×10^{2}
2117	0.1690	302.0	1.175	4.864	4.084
3788	0.03508	200.8	3.67×10^{-8}	4.914	1.294×10^{3}
10100	2.475×10^{-3}	100.8	5.158×10^{-9}	4.964	9.119
17320	5.765×10^{-4}	69.0	1.755	4.979	2.671×10^{4}

Table III

θ = 0.3 Radians

x(cm)	p	T	ρ	u	A
143.8	125.4	1417	1.86×10^{-5}	4.17×10^{5}	3.010
169.1	83.52	1310	1.34	4.253	4.098
199.5	54.89	1202	9.590×10^{-6}	4.330	5.622
234.4	36.15	1102	6.891	4.399	7.701
274.7	24.12	1009	5.021	4.461	1.042×10^{1}
333.9	14.61	902.7	3.400	4.529	1.516
404.7	8.877	805.5	2.315	4.588	2.198
508.2	4.895	700.6	1.468	4.649	3.420
636.5	2.706	607.6	9.359×10^{-7}	4.702	5.305
856.6	1.230	500.3	5.168	4.760	9.490
1193	0.5078	400.2	2.666	4.813	1.819×10^{2}
1782	0.1723	303.1	1.194	4.862	4.021
3189	0.03578	201.6	3.729×10^{-8}	4.913	1.274×10^{3}
8507	2.524×10^{-3}	101.2	5.24×10^{-9}	4.963	8.978
14590	5.869×10^{-4}	69.3	1.78	4.979	2.634×10^{4}

Table IV

θ = 0.8 Radians

x(cm)	p	T	ρ	u	A
46.79	125.4	1417	1.86×10^{-5}	4.17×10^{5}	3.010
54.78	84.51	1309	1.356	4.251	4.049
64.17	56.73	1206	9.885×10^{-6}	4.325	5.460
75.06	38.12	1108	7.226	4.392	7.356
87.68	25.64	1017	5.296	4.453	9.899
106.3	15.64	911.4	3.605	4.520	1.433×10^{1}
128.6	9.546	814.4	2.463	4.579	2.070
161.2	5.267	709.3	1.566	4.641	3.212
201.8	2.929	615.6	9.996×10^{-7}	4.694	4.975
261.7	1.471	519.9	5.947	4.747	8.271
364.4	0.6075	416.3	3.066	4.802	1.586×10^{2}
544.7	0.2061	315.6	1.372	4.853	3.505
940.1	0.04723	215.4	4.607×10^{-8}	4.904	1.033×10^{3}
2249	4.469×10^{-3}	116.7	8.050×10^{-9}	4.953	5.856×10^{3}
4793	5.784×10^{-4}	68.6	1.772	4.976	2.648×10^{4}

Table V

Saturation Conditions

	θ = 0.0	θ = 0.3	θ = 0.8
x(cm)	3225	2720	860
T(°K)	225	225	229
p (torr)	0.054	0.055	0.060
p_{H_2O} (torr)	0.038	0.038	0.042
M	11.16	11.15	11.14
u (cm/sec)	490100	489700	493600
A/A*	1854	1845	1837

Table VI

Summary of Input Conditions

	$\theta = 0.0$	$\theta = 0.3$	$\theta = 0.8$
p_o (torr)	9249	9318	9485
T_o (°K)	5146	5142	5138
ω_o	0.9527	0.9527	0.9527
μ_i	2.016	2.016	2.016
μ_v	18.016	18.016	18.016
γ_i	1.403	1.403	1.403
γ_v	1.332	1.332	1.332
A^* (cm^2)	0.5058	0.5021	0.4926
C (cm^{-2})(a)	1.783×10^{-4}	2.495×10^{-4}	2.373×10^{-3}

(a) For $A/A^* = Cx^2$

Table VII

Computed conditions at onset, using $\Gamma = 10^5$, classical steady-state homogeneous nucleation theory with $\sigma = \sigma_\infty$

	$\theta = 0.0$	$\theta = 0.3$	$\theta = 0.8$
x (m)	47.0	39.6	13.0
p (torr)	0.0195	0.0199	0.0195
p_{H_2O} (torr)	0.0135	0.0138	0.0135
T (°K)	173	173	171
A/A*	3940	3910	4010
M	12.8	12.8	12.9
s_{cr}	~1500	~1450	~2000
r*(Å)	3.6	3.6	3.5
n*	6	6	6
N (cm^{-3})	$\sim 10^{10}$	$\sim 10^{10}$	$\sim 10^{10}$

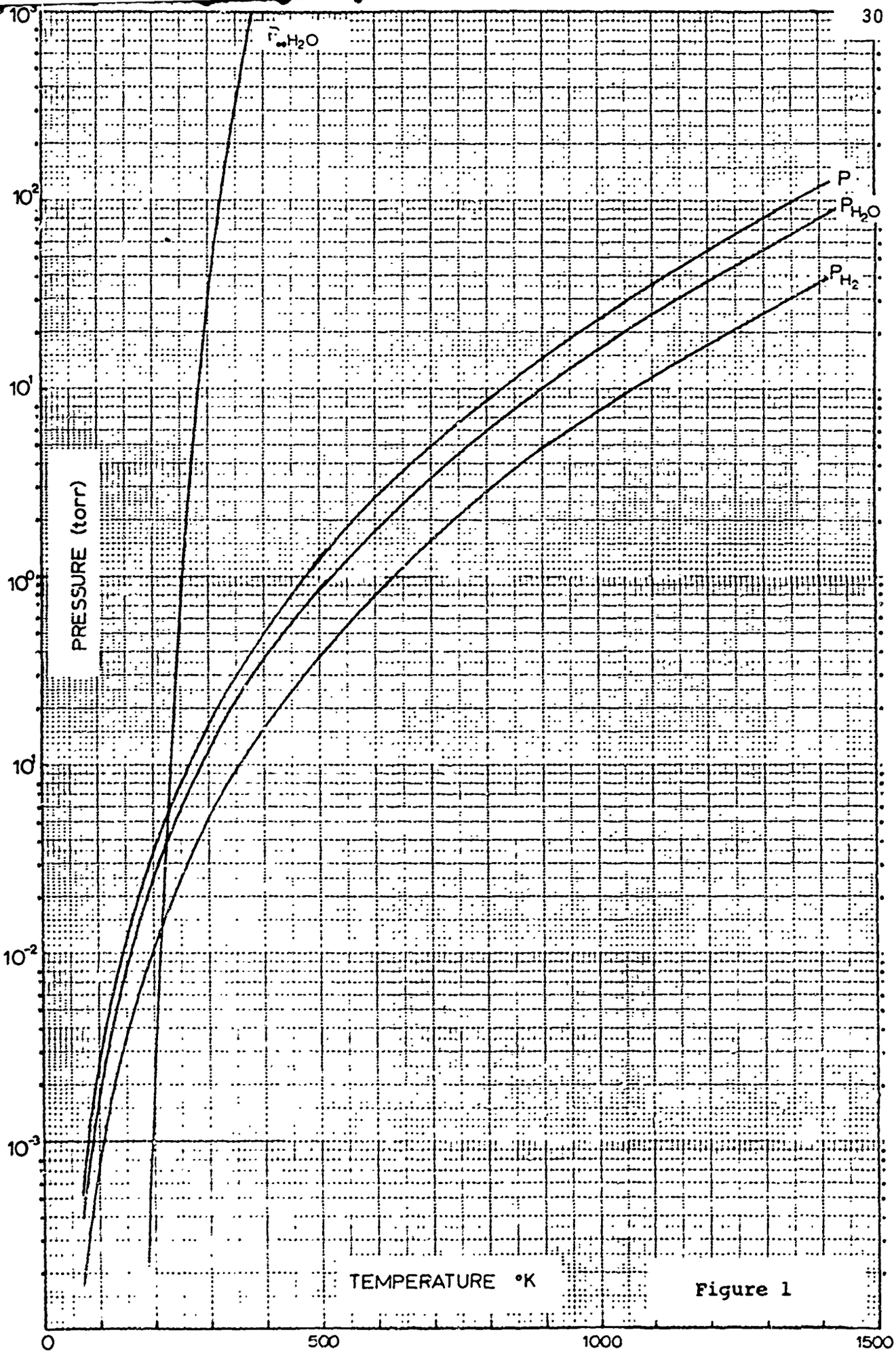
$P_{\infty H_2O}$
P
P_{H_2O}
P_{H_2}
PRESSURE (torr)
10^{2}
10^{1}
10^{0}
10^{-1}
10^{-2}
10^{-3}
0
500
1000
1500
TEMPERATURE °K

Figure 1

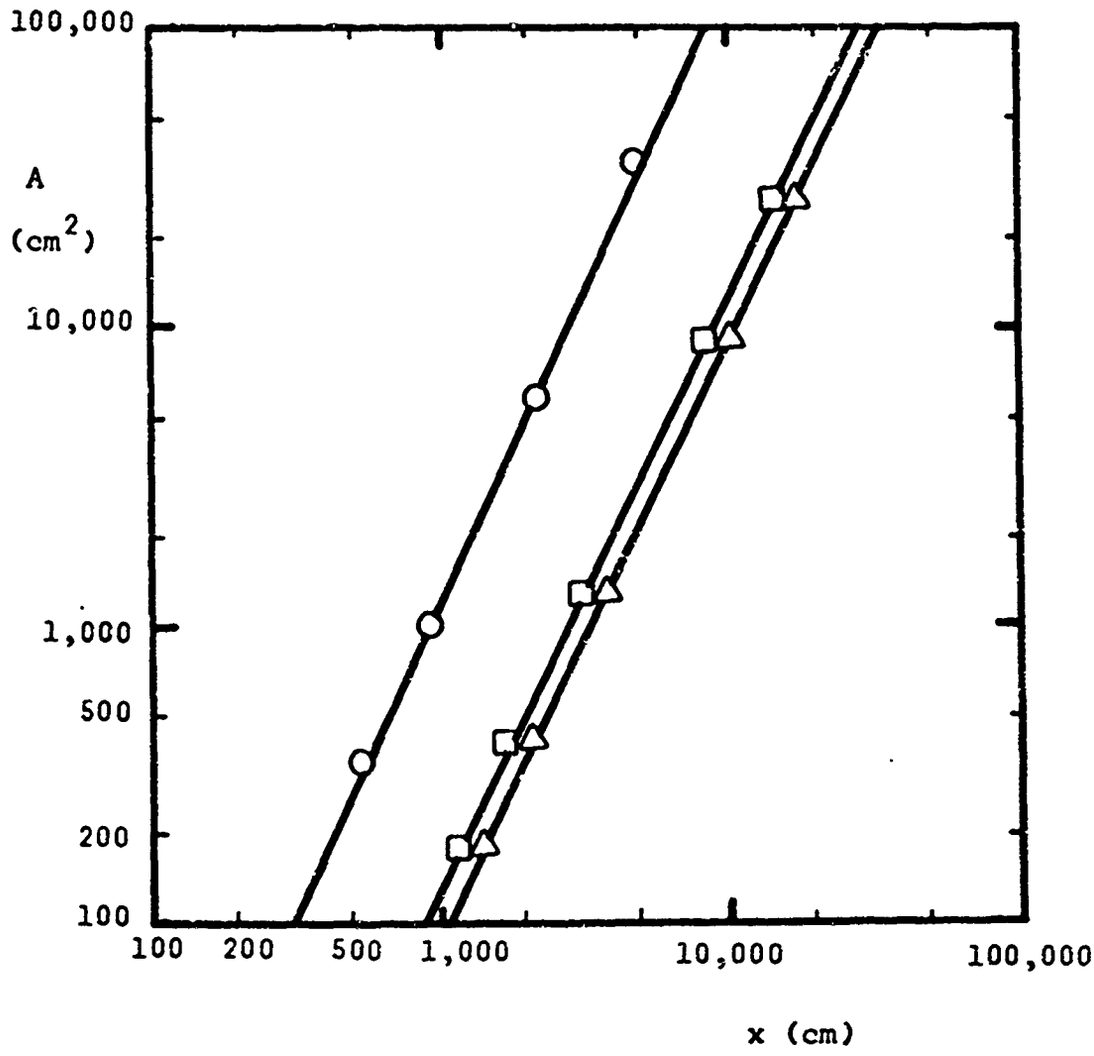
100,000
A
(cm²)
10,000
1,000
500
200
100
100
200
500
1,000
10,000
100,000
x (cm)

Figure 2

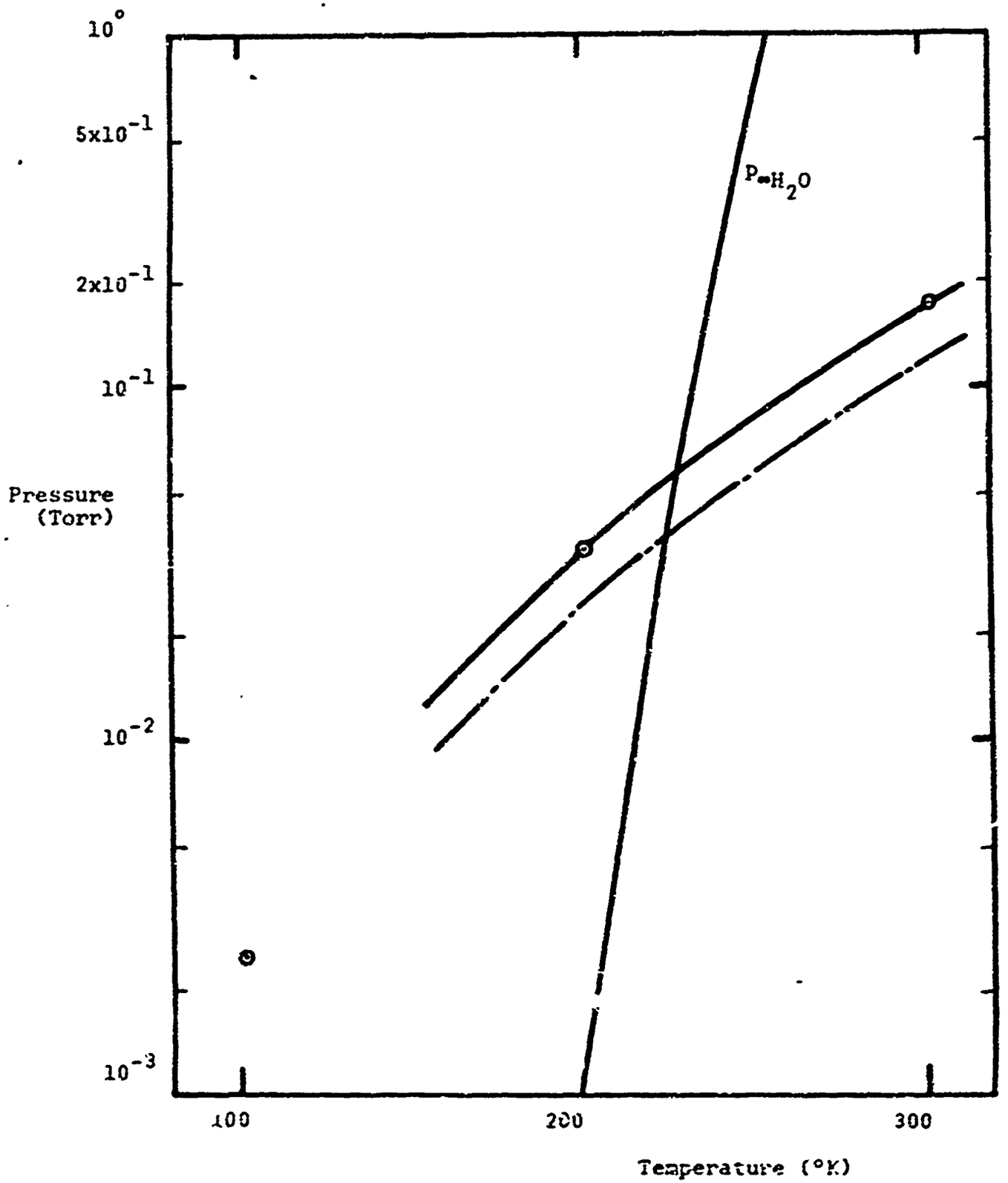
10°
5x10⁻¹
2x10⁻¹
10⁻¹
10⁻²
10⁻³
Pressure (Torr)
P=H2O
100
200
300
Temperature (°K)

Figure 3

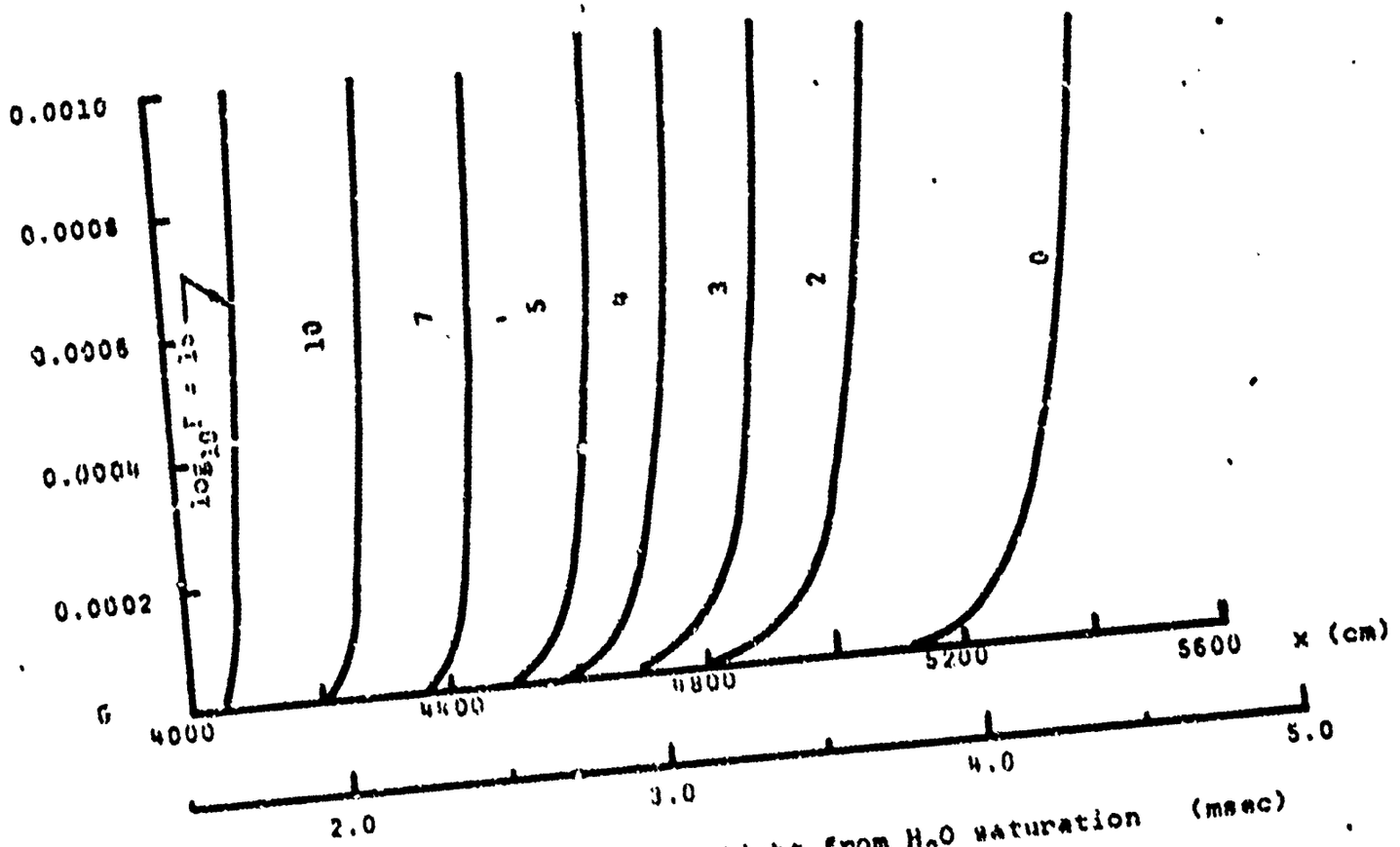
0.0010
0.0008
0.0006
0.0004
0.0002
G
10
7
5
4
3
2
0
4000
4400
4800
5200
5600
x (cm)
2.0
3.0
4.0
5.0
Time of flight from H_2O saturation (msec)

Figure 4

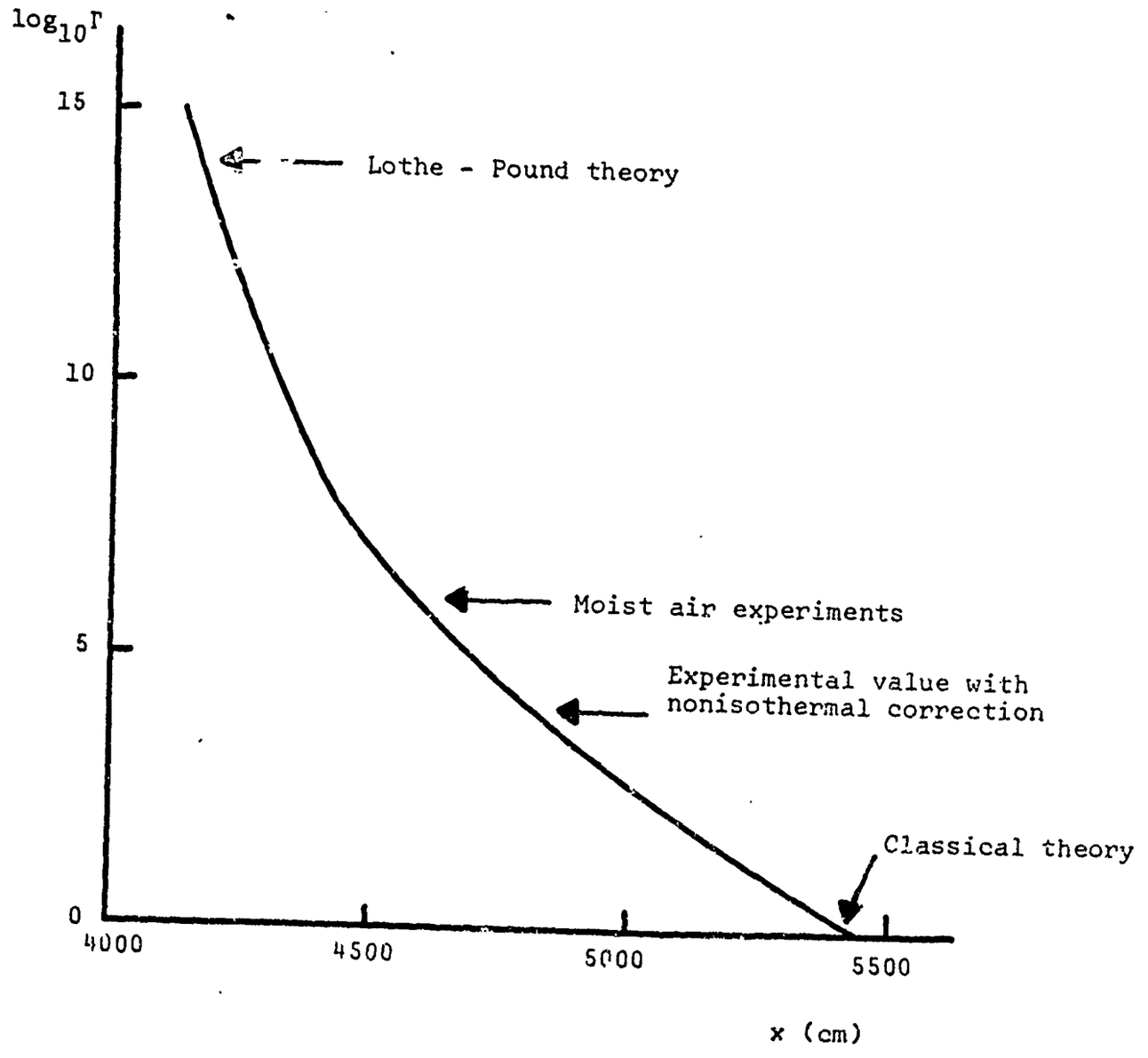
$\log_{10}\Gamma$
15
10
5
0
4000
4500
5000
5500
x (cm)
Lothe - Pound theory
Moist air experiments
Experimental value with nonisothermal correction
Classical theory

Figure 5

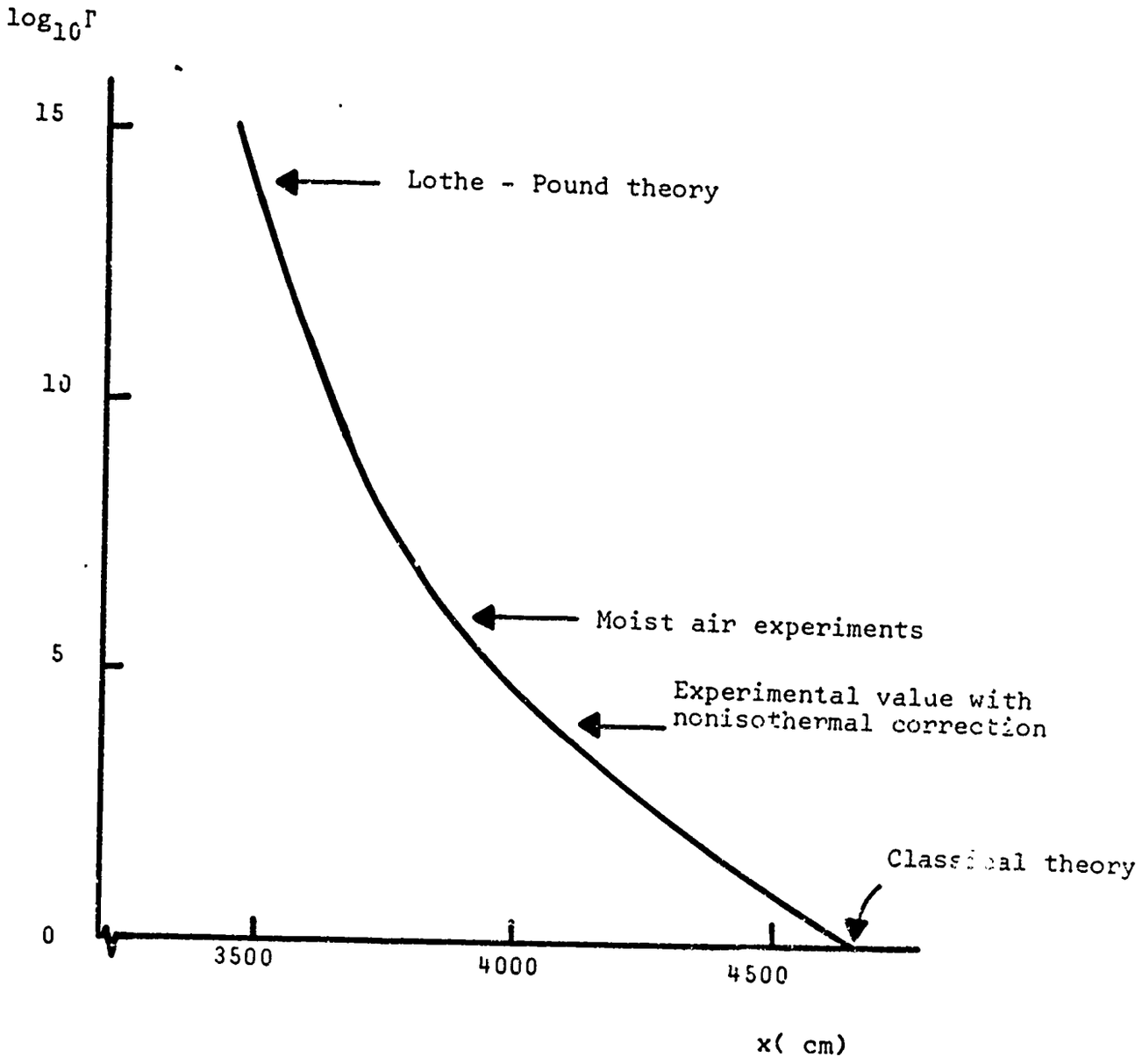
$\log_{10}\Gamma$
15
10
5
0
3500
4000
4500
x(cm)
Lothe - Pound theory
Moist air experiments
Experimental value with
nonisothermal correction
Classical theory

Figure 6

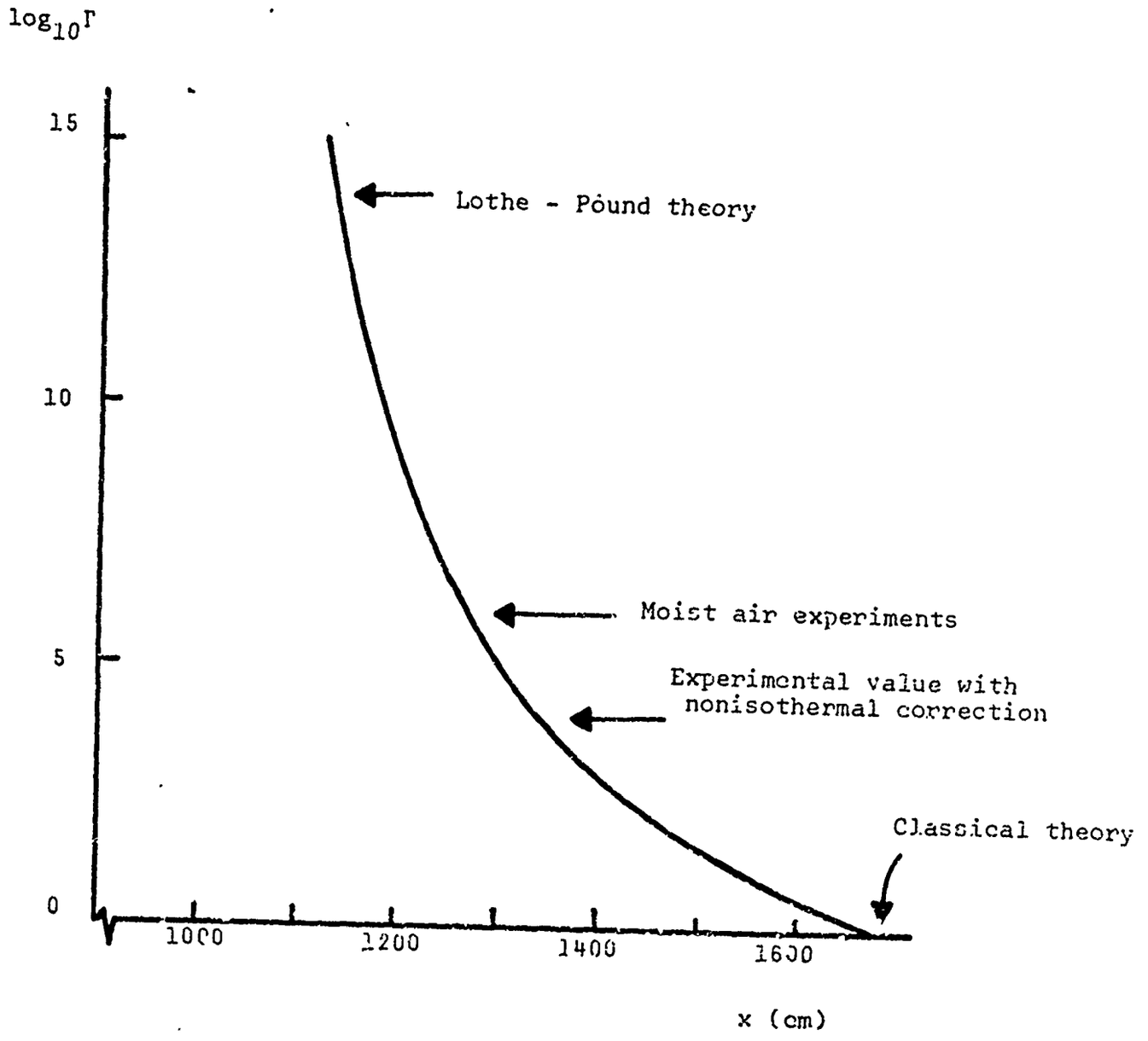
$\log_{10}\Gamma$
15
10
5
0
Lothe - Pound theory
Moist air experiments
Experimental value with nonisothermal correction
Classical theory
1000
1200
1400
1600
x (cm)

Figure 7

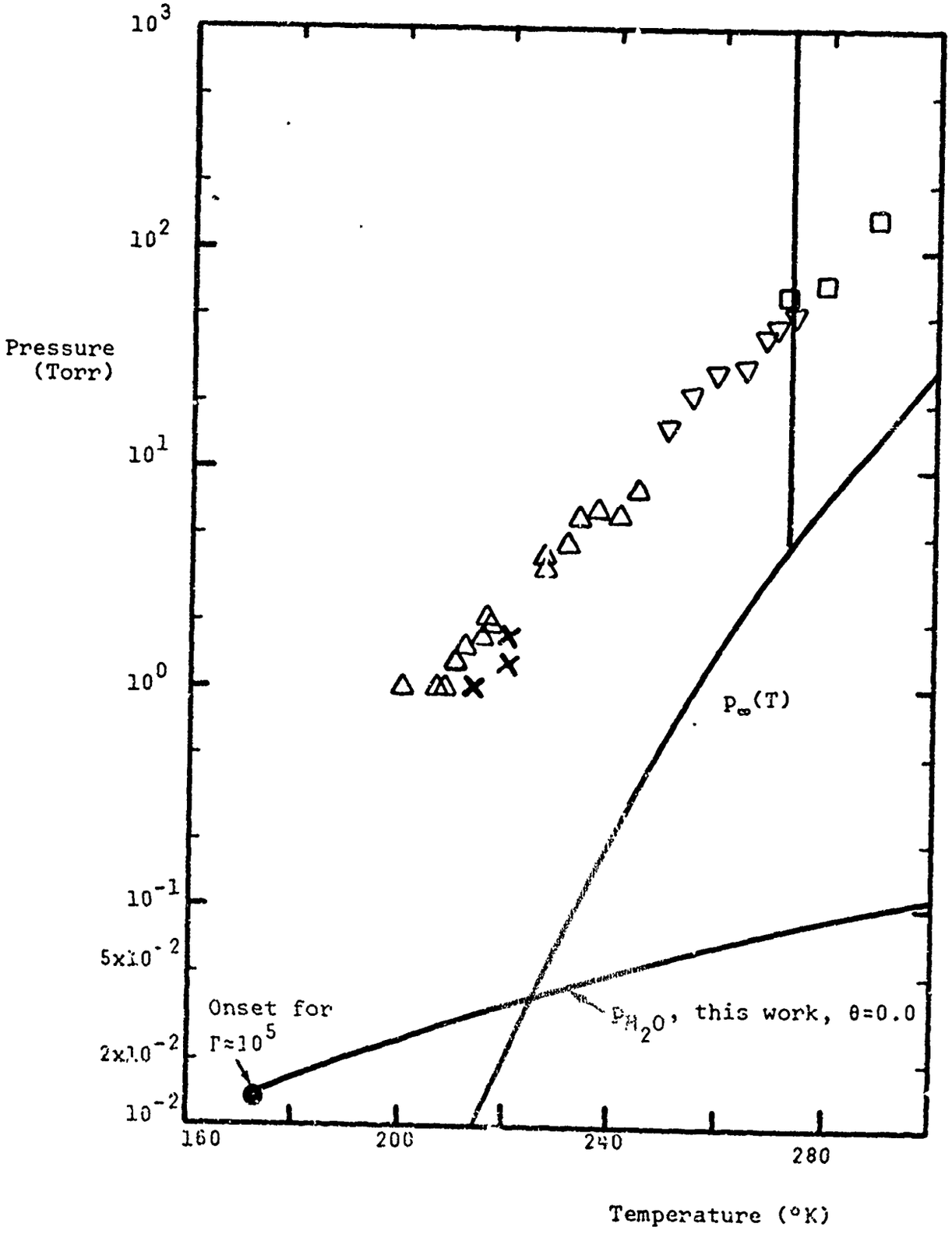
10^3
10^2
Pressure
(Torr)
10^1
10^0
10^{-1}
$5x10^{-2}$
$2x10^{-2}$
10^{-2}
$p_\infty(T)$
Onset for
$\Gamma \approx 10^5$
p_{H_2O}, this work, θ=0.0
160
200
240
280
Temperature (°K)

Figure 8

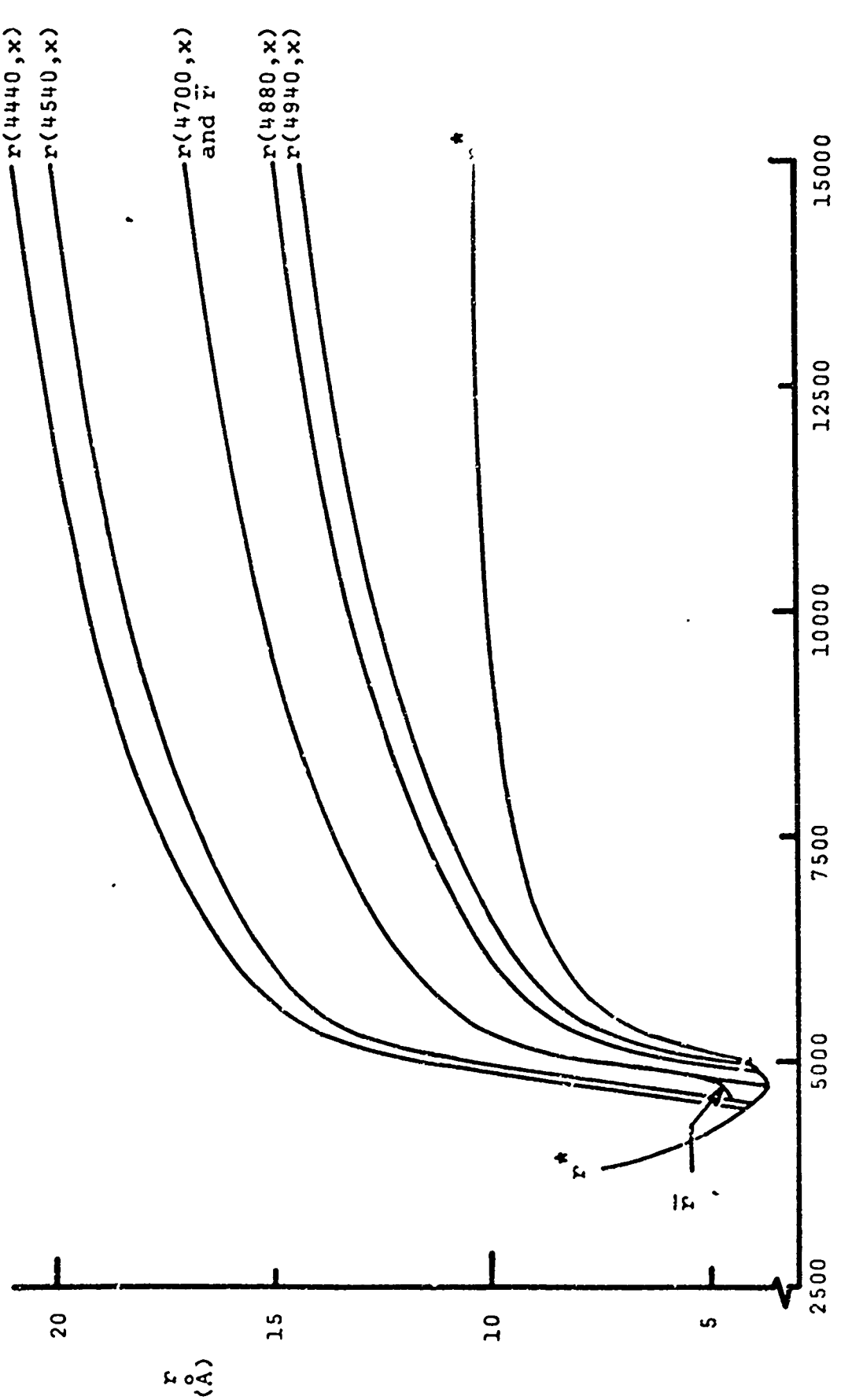
r(4440,x)
r(4540,x)
r(4700,x)
and r̄
r(4880,x)
r(4940,x)
r*
r̄
20
15
10
5
r
(Å)
2500
5000
7500
10000
12500
15000
x (cm)

Figure 9